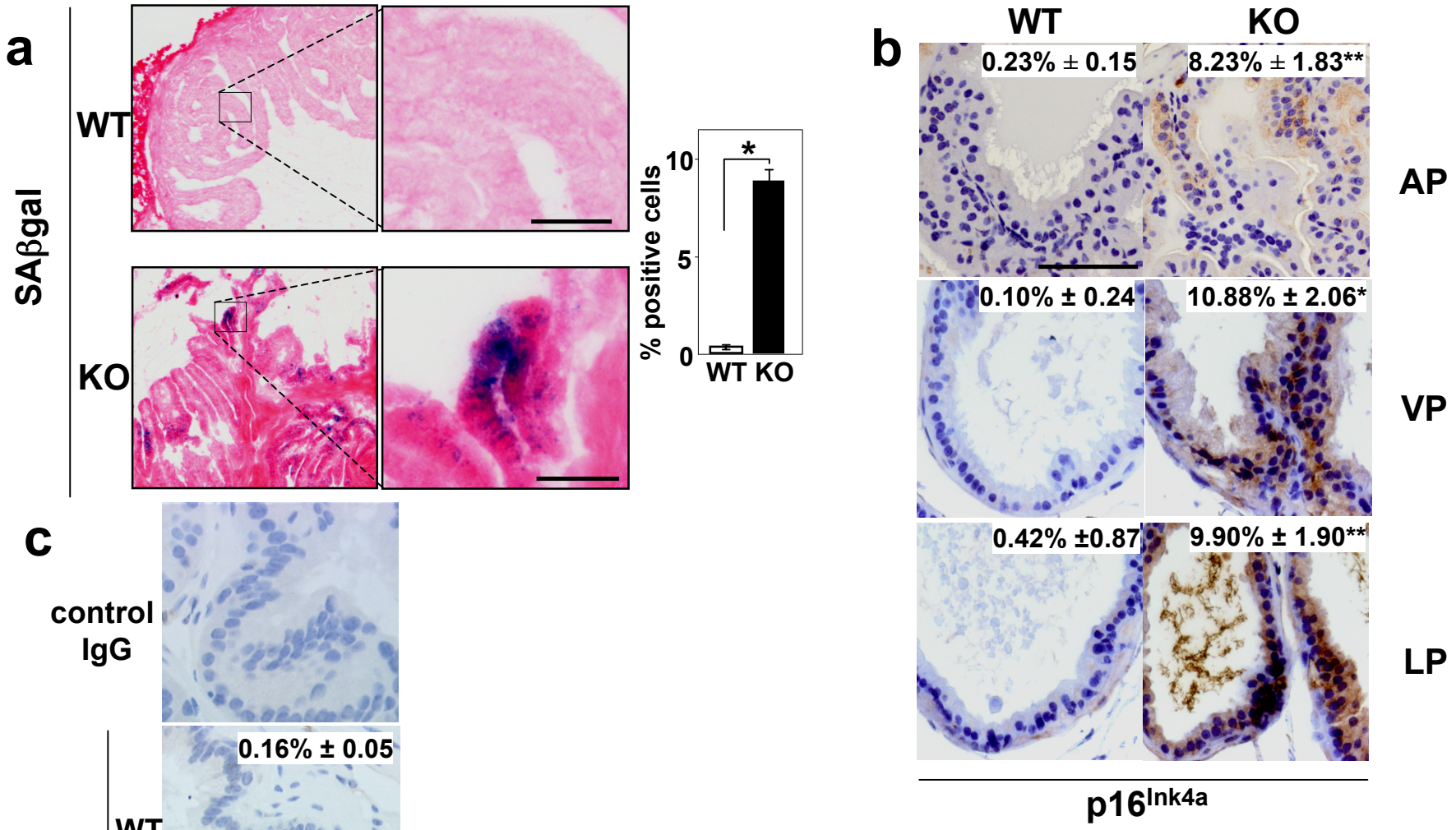

Supplement Fig. S1 Increased expression of senescence markers in the hyperplastic prostates of *akap12*-null mice. **(a)** Anterior prostate lobes from age-matched (4 mo) WT or KO male mice stained for SAβgal and eosin. The percentage of SAβgal-positive cells in high magnification fields is shown at right. Error bars, S.E. in 8 fields/analysis (at least 100 cells/field); *, $p<0.001$. **(b)** Anterior (AP), ventral (VP), or lateral (LP) prostate lobes from WT or KO mice stained for $p16^{Ink4a}$ and counterstained with Mayer's hematoxylin. **(c)** AP from WT or KO male mice stained for γH2AX (bottom two panels) or control IgG (top panel). The percentage of γH2AX- or $p16^{Ink4a}$-positive cells in high magnification fields is shown in inset panels, based on averages with S.E. of 8 fields/analysis (at least 100 cells/field). *, P<0.001; **, P<0.005. Size bars, 50 μm.

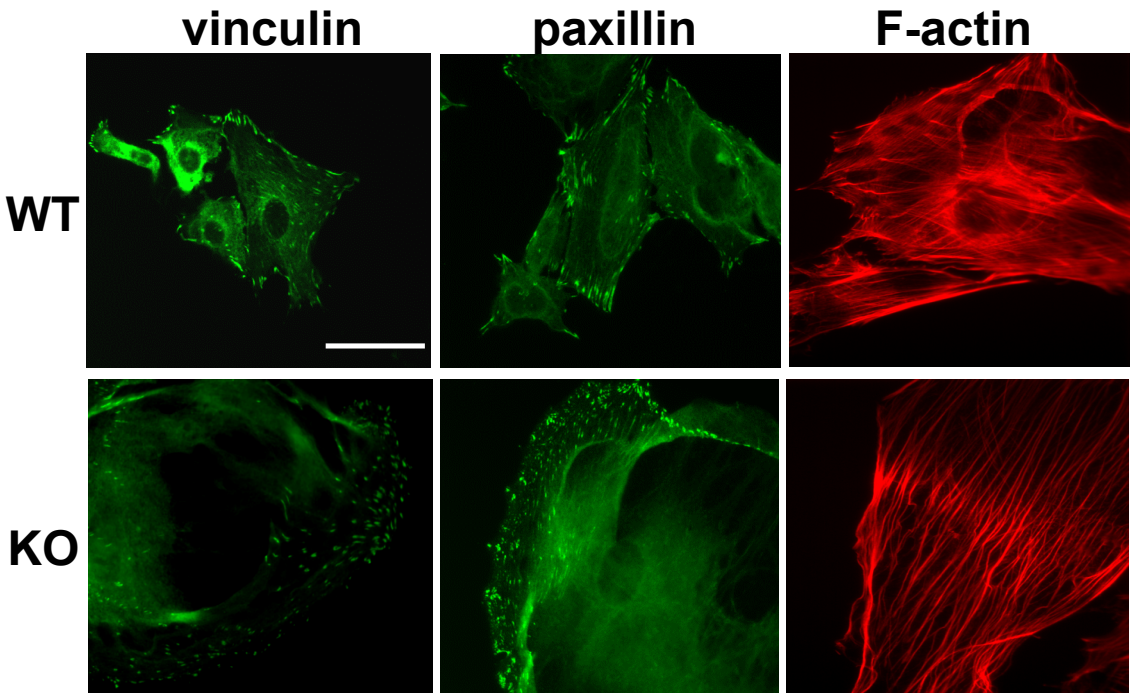

Supplemental Fig. S2. Increased dorsal focal adhesion plaque and longitudinal stress fiber formation in *akap12*-null MEF. WT- or KO-MEF stained for vinculin, paxillin, or F-actin as described in the Materials and Methods. Size bar, 10 μm.

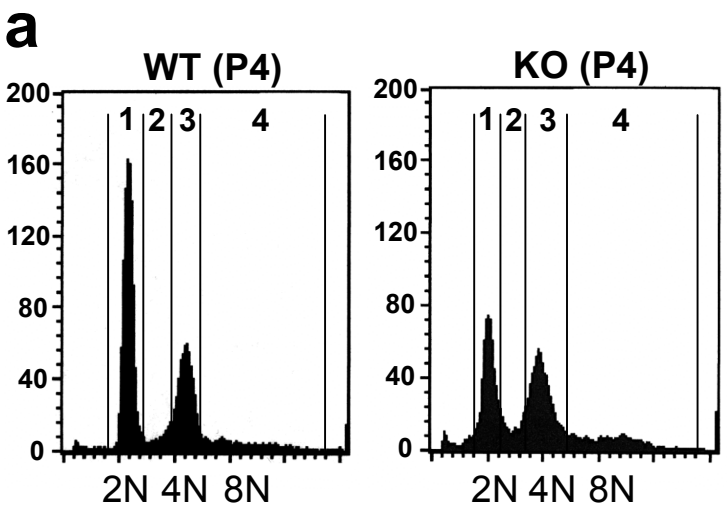

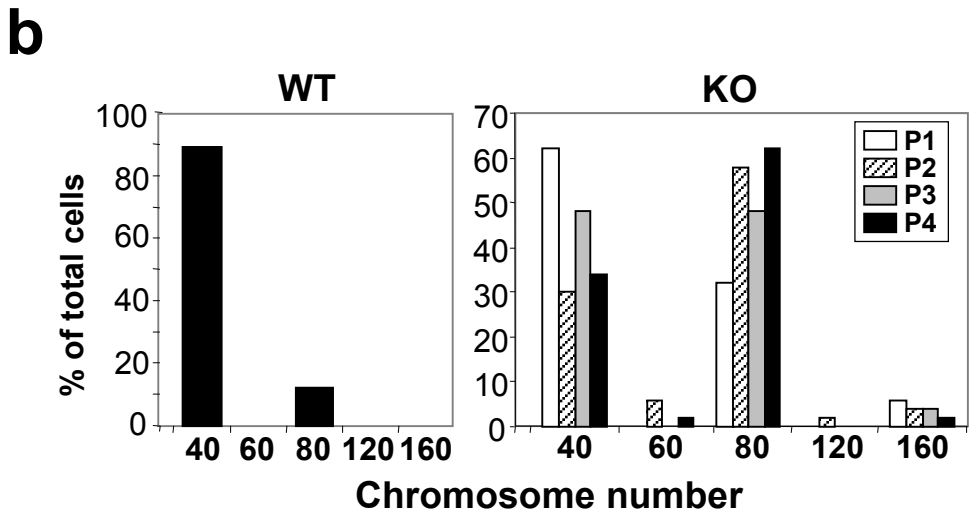

		WT	KO
1	G0/G1	65.4	36.5
2	S	4.4	7.1
3	G2/M	21.5	40.3
4	polyploidy	6.7	14.1

Supplemental Fig. S3. Loss of Akap12 leads to multinucleation and polyploidy. **(a)** Total DNA content in passage 4 (P4) WT- vs. KO-MEF after cytometric analysis of PI-stained cells. **(b)** Number of chromosomes/cell WT- (P4) or KO-MEF (P1-P4) based on counting at least 100 nuclei per cell type from colcemid-induced metaphase spreads.

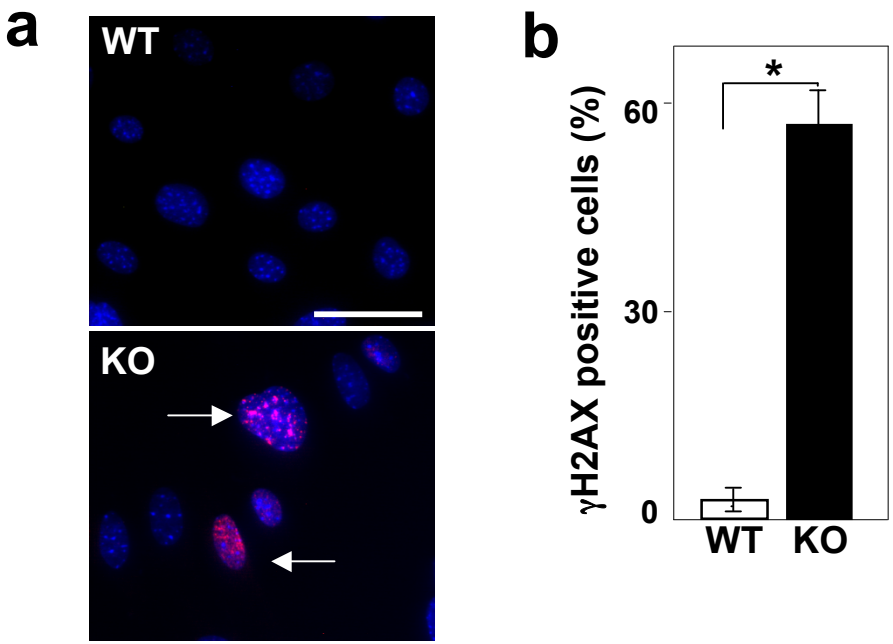

Supplemental Fig. S4. KO-MEF exhibit increased levels of the DNA damage marker, γH2AX. **(a)** Passage-matched (P7) WT- or KO-MEF stained for γH2AX. Arrows, intranuclear senescence associated γH2AX-positive foci. Size bar = 20 μm. (**b**) Percentage of γH2AX-positive cells from panel A. Error bars, S.E. from eight independent microscopic fields containing at least 35 cells/field. **, p*<0.001.

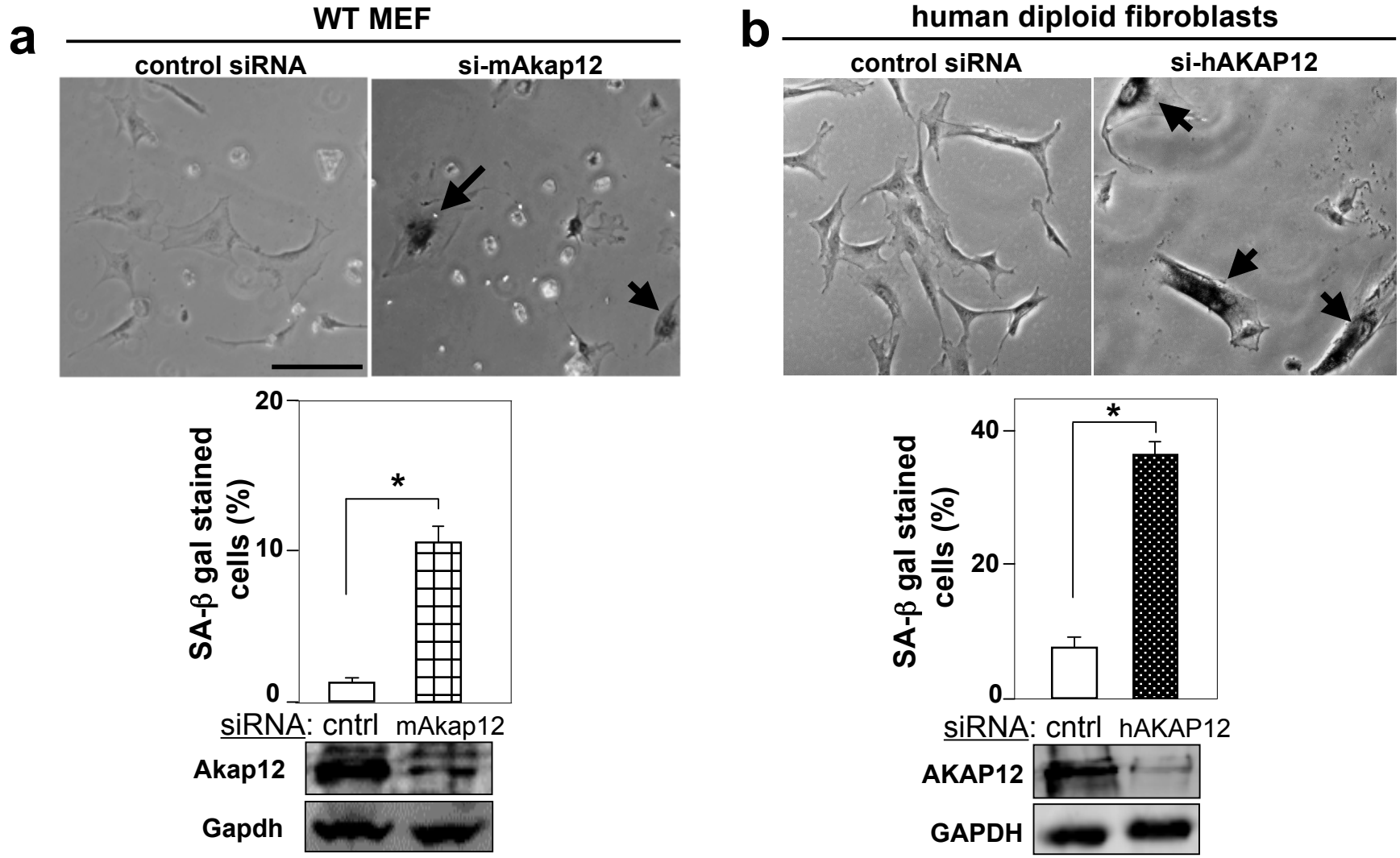

Supplemental Fig. S5. RNAi-mediated knockdown of AKAP increases senescence in diploid fibroblasts. *Upper panels*- Phase contrast images of WT-MEF **(a)** or human diploid fibroblasts **(b)** treated with scrambled ("control") siRNA (left) or AKAP12-specific siRNA (right). Arrows, SAβgal stained cells. Size bar = 30 μm. *Middle panels*- percentage of SAβgal stained cells. Error bars, S.E. from eight microscopic fields containing at least 50 cells/field. *, $p<0.005$. *Bottom panels*- Immunoblotting analysis probing for AKAP12 or GAPDH in the cells treated with scrambled ("cntrl") or AKAP12-specific siRNA.

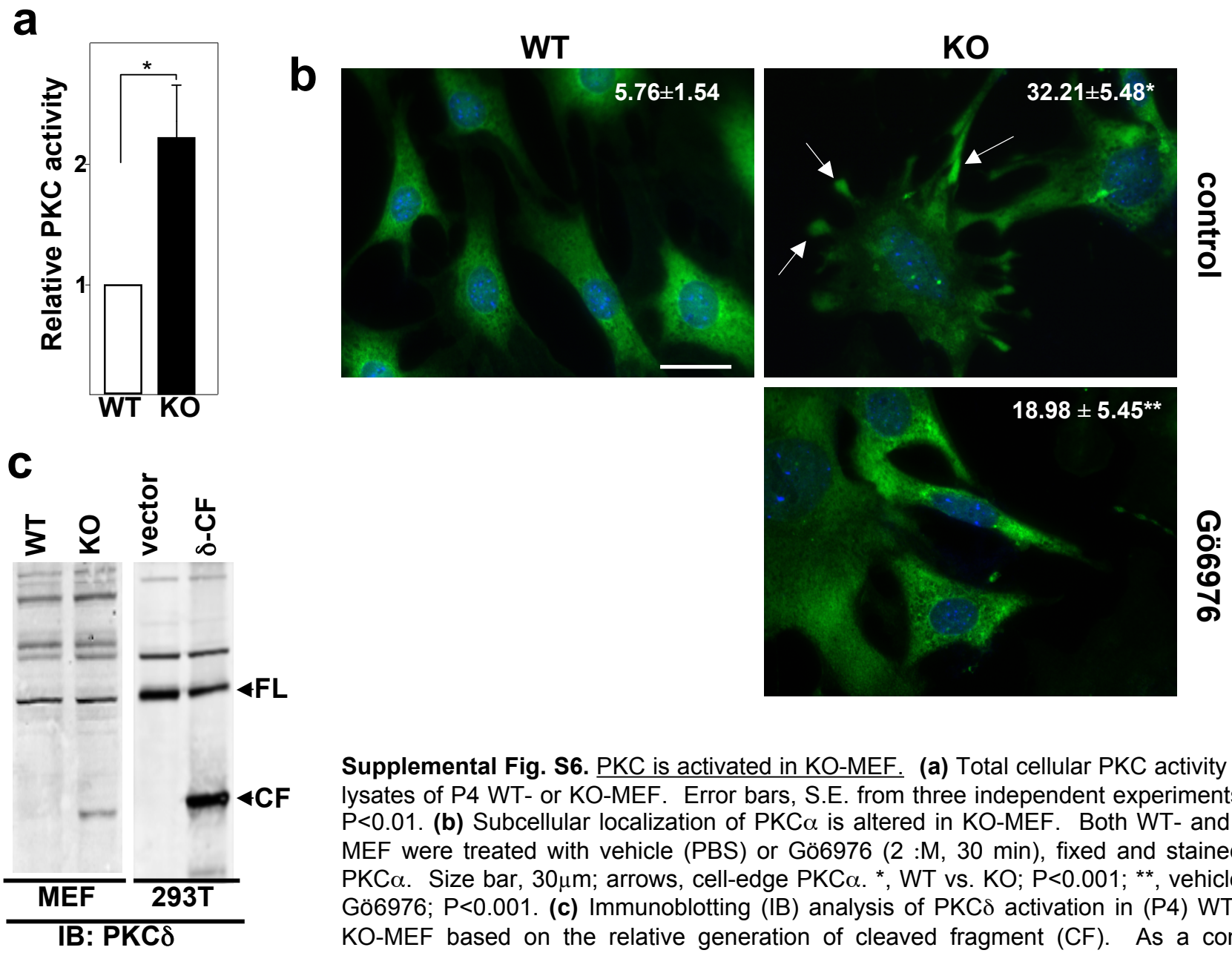

Supplemental Fig. S6. PKC is activated in KO-MEF. **(a)** Total cellular PKC activity from lysates of P4 WT- or KO-MEF. Error bars, S.E. from three independent experiments. *, P<0.01. **(b)** Subcellular localization of PKCα is altered in KO-MEF. Both WT- and KO-MEF were treated with vehicle (PBS) or Gö6976 (2 :M, 30 min), fixed and stained for PKCα. Size bar, 30μm; arrows, cell-edge PKCα. *, WT vs. KO; P<0.001; **, vehicle vs. Gö6976; P<0.001. **(c)** Immunoblotting (IB) analysis of PKCδ activation in (P4) WT- vs. KO-MEF based on the relative generation of cleaved fragment (CF). As a control, HEK293T cells were transiently transfected with a PKCδ-CF (40 kDa) expression vector or empty vector. FL, full length; CF, cleaved fragment.

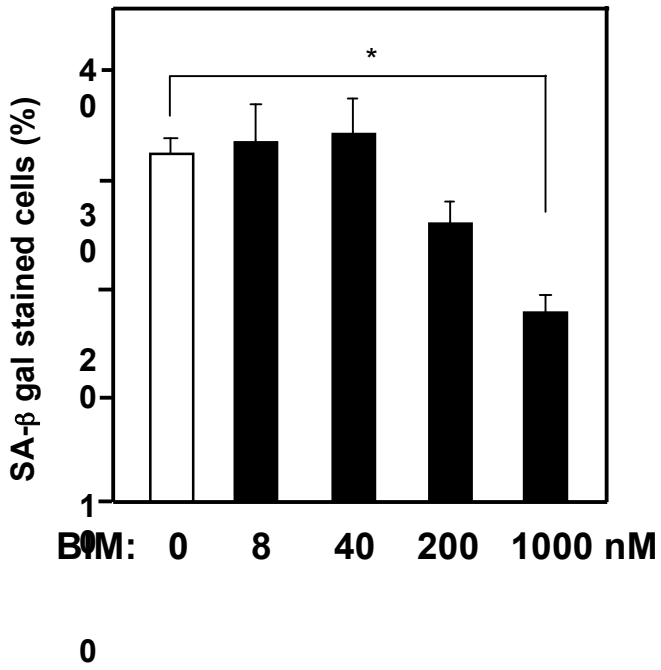

Supplemental Fig. S7. Premature senescence in KO-MEF correlates with PKC kinase activity. Percentage of SAβgal-stained KO-MEF treated for 16 hrs with various concentrations of *bis*-indolylmaleimide (BIM). The data are from at least four independent experiments. Error bars, S.E., *, P<0.005

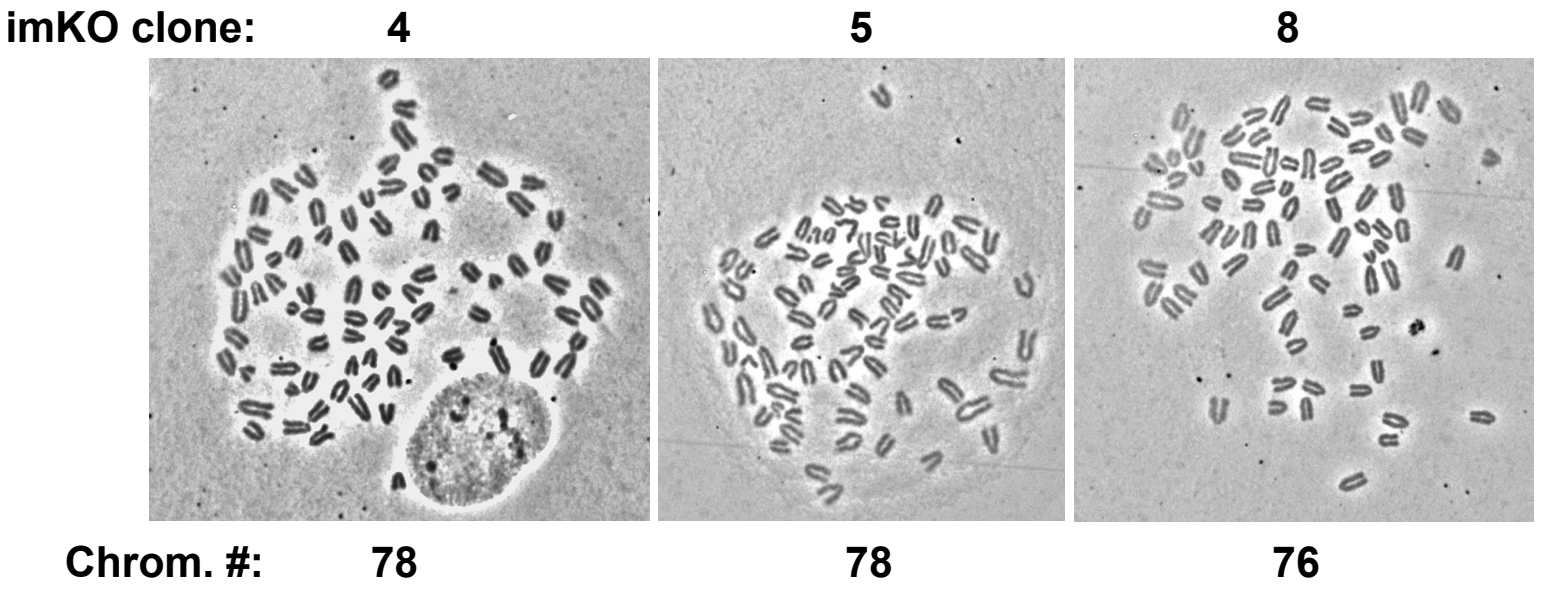

Supplemental Fig. S8. imKO clones contain slightly sub-tetraploid genomes. Karyotype analyses of metaphase spread cells show slightly under the tetraploid number of 80 chromosomes/cell in several independently-derived imKO clones.

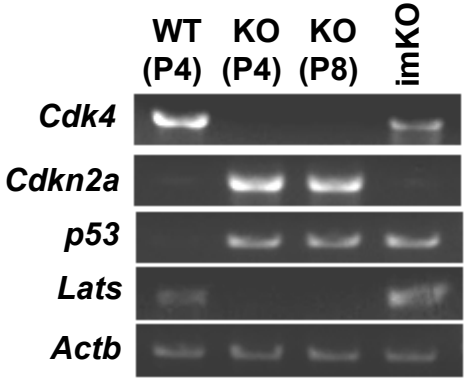

1.0	0.01 ± 0.01	0.1 ± 0.03	0.9 ± 0.1
1.0	6.8 ± 1.0	6.1 ± 1.2	1.1 ± 0.2
1.0	3.2 ± 0.8	3.0 ± 0.8	3.4 ± 0.8
1.0	0.2 ± 0.1	0.1 ± 0.1	1.5 ± 0.2
1.0	1.0	1.0	1.0

Supplemental Fig. S9. Loss of senescence-associated gene signature in imKO cells. Semi-Q RT-PCR analysis of Cdk4, $p16^{Ink4a}$, p53, and Lats1 transcript levels using WT-MEF, pre-senescent (P4) and late-senescent (P8) KO-MEF and immortalized KO-MEF (imKO).

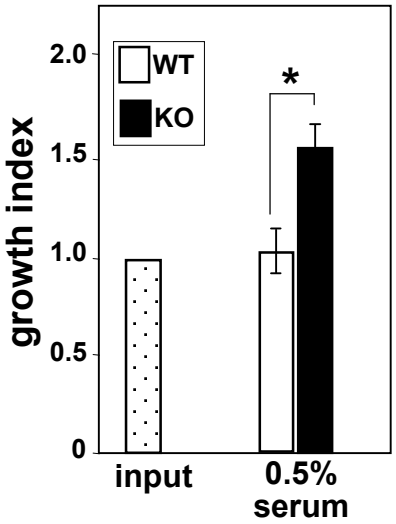

Supplemental Fig. S10. KO-MEF exhibit serum-independent growth. Relative proliferation (growth index) of P6 WT- or KO-MEF cultured for 48h in DMEM containing 0.5% FBS. Input, starting number of seeded cells (5 x 10^5/10-cm dish). Error bars, S.E. of triplicates from two independent experiments. *, $P<0.05$.

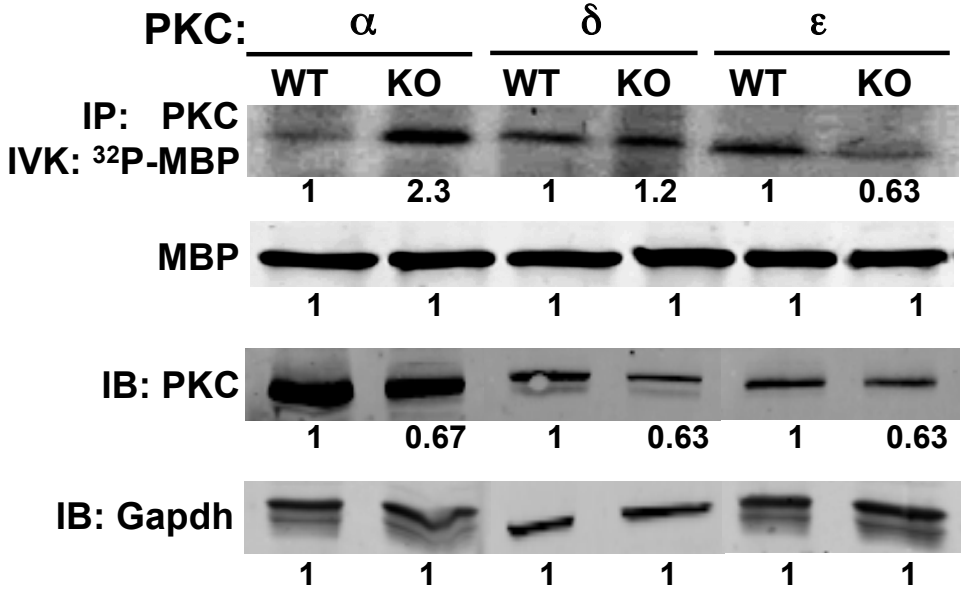

Supplemental Fig. S11. Relative PKCΑ, ∗, and , specific activities in WT- vs. KO-MEF (data used to generate Fig. 3b). PKC isozymes were IP'ed from P4 MEF lysates using isozyme-specific Abs, then added to *in vitro* kinase reactions containing myelin basic protein (MBP) substrate plus ^{32}P-ATP. The labeled substrate was detected by phosphorimaging (top panel) and by Coomassie staining ("MBP"), whereas the relative PKC protein levels were determined by IB using Gapdh controls. The relative protein or phospho-substrate levels were determined by densitometry, and the relative PKC isozyme activity was calculated as the relative ^{32}P-MBP levels normalized to total MBP, PKC isozyme and Gapdh protein levels. This image is typical of three independent experiments with <20% variations between the same samples.